Copyright © 2018 Tech Science Press CMC, vol.57, no.1, pp.123-144, 2018

Dynamical Interaction Between Information and Disease Spreading in Populations of Moving Agents

Lingling Xia[1], Bo Song[2, 3], Zhengjun Jing[4], Yurong Song[5, *] and Liang Zhang[1]

Abstract: Considering dynamical disease spreading network consisting of moving individuals, a new double-layer network is constructed, one where the information dissemination process takes place and the other where the dynamics of disease spreading evolves. On the basis of Markov chains theory, a new model characterizing the coupled dynamics between information dissemination and disease spreading in populations of moving agents is established and corresponding state probability equations are formulated to describe the probability in each state of every node at each moment. Monte Carlo simulations are performed to characterize the interaction process between information and disease spreading and investigate factors that influence spreading dynamics. Simulation results show that the increasing of information transmission rate can reduce the scale of disease spreading in some degree. Shortening infection period and strengthening consciousness for self-protection by decreasing individual's scope of activity both can effectively reduce the final refractory density for the disease but have less effect on the information dissemination. In addition, the increasing of vaccination rate or decreasing of long-range travel can also reduce the scale of disease spreading.

Keywords: Complex networks, Markov chains theory, interaction process, spreading dynamics, double-layer network.

1 Introduction

When disease spreads among humans, information about disease also spreads like infections within populations. Information dissemination can arouse the changes of human behavior in epidemic propagation while these behavioral changes in turn influence and even change disease dynamics. For example, individuals may decide to avoid infected individuals, or get vaccinated after hearing about the disease [Rizzo, Frasca and Porfiri (2014)]. Disease spreading and information dissemination have become two fundamental and interdependent dynamical processes on complex networks, which has led to a new

[1] Department of Computer Information and Cyber Security, Jiangsu Police Institute, Nanjing, 210031, China.

[2] College of Telecommunications and Information Engineering, Nanjing University of Posts and Telecommunications, Nanjing, 210003, China.

[3] Global Big Data Technologies Centre, University of Technology Sydney, Sydney, 2007, Australia.

[4] College of Computer Engineering, Jiangsu University of Technology, Changzhou, 213001, China.

[5] College of Automation, Nanjing University of Posts and Telecommunications, Nanjing, 210003, China.

[*] Corresponding Author: Yu-Rong Song. Email: songyr@njupt.edu.cn.

direction of research, that is, the research on dynamical interaction between the two types of spreading dynamics [Wang, Tang, Yang et al. (2014)].

To understand how information dissemination can change human behavior that is responsive to the presence of a disease, and further affect epidemic outbreaks, more and more researchers begin to investigate the influence of information dissemination on the disease spreading by incorporating human behavior into disease models [Wang, Tang, Yang et al. (2014); Bagnoli, Lio and Sguanci (2007); Fenichel, Castillo-Chavez, Ceddia et al. (2011); Chen, Jiang, Rabidoux et al. (2011); Zhang, Xie, Tang et al. (2014); Epstein, Parker, Cummings et al. (2008); Perra, Balcan, Gonçalves et al. (2011); Sahneh and Scoglio (2012); Ruan, Tang and Liu (2012); Liu, Xie, Chen et al. (2015); Funk, Gilad, Watkins et al. (2009); Granell, Gómez and Arenas (2013); Granell, Gómez and Arenas (2014)]. There are three main approaches to model the behavioral changes, namely, by modifying infectivity or contact rates [Bagnoli, Lio and Sguanci (2007); Fenichel, Castillo-Chavez, Ceddia et al. (2011); Chen, Jiang, Rabidoux et al. (2011); Zhang, Xie, Tang et al. (2014)], introducing additional classes or compartments in epidemiological models [Epstein, Parker, Cummings et al. (2008); Perra, Balcan, Gonçalves et al. (2011); Sahneh and Scoglio (2012); Ruan, Tang and Liu (2012); Liu, Xie, Chen et al. (2015)], and defining coupled models between disease spreading and information dissemination [Wang, Tang, Yang et al. (2014); Funk, Gilad, Watkins et al. (2009); Granell, Gómez and Arenas (2013); Granell, Gómez and Arenas (2014)]. In the first two approaches, researchers pay more attention on exploring and analyzing the influence of human behaviors on epidemic dynamics and neglect the influence of information dynamics. Moreover, the network model that supports spreading dynamics is characterized based on the structure of single layer complex network. In fact, the propagation mechanism and underlying network of information are different from that of disease. Information is often disseminated and exchanged through electronic communication networks, such as telephones [Jiang, Xie, Li et al. (2013)], instant messaging system (IMS), and the social networking service (SNS), but disease spreading usually takes place on a physical contact network [Starnini, Baronchelli and Pastor-Satorras (2013)]. Consequently, the third approach by defining coupled models between the two types of spreading dynamics has been given more attention in recent years.

A pioneering step was taken by Funk et al. [Funk, Gilad, Watkins et al. (2009)], who linked information transmission model to an epidemiological susceptible-infected-recovered (SIR) model to investigate how the spread of awareness influences disease spreading. Information dissemination makes people who aware of a disease in their proximity take measures to reduce their susceptibility, which leads to a lower size of the disease outbreak in a well-mixed population but does not affect the epidemic threshold. Considering the difference in the epidemic and information spreading processes, Granell et al. [Granell, Gómez and Arenas (2013)] proposed the use of microscopic Markov chain approach (MMCA) to understand the dynamical interaction in multiplex networks where the nodes represent the same entities in all layers. The multiplex corresponds to a double-layer network, one where the unaware-aware-unaware (UAU) process takes place and the other where the dynamics of susceptible-infected-susceptible (SIS) evolves. The analysis of the interrelation between two processes on top of multiplex networks revealed the existence of a metacritical point at which the dissemination of awareness is able to

control the onset of the epidemics. Later, Granell et al. [Granell, Gómez and Arenas (2014)] proposed a full analysis of the critical properties in the more general scenario where infection does not imply immediate awareness, and where awareness dissemination does not imply total immunization. They further analyzed the influence of a massive broadcast of awareness (mass media) on the final outcome of the epidemic and found that the presence of the mass media makes the metacritical point vanish. Wang et al. [Wang, Tang, Yang et al. (2014)] investigated the asymmetrical interplay between the two intimately related dynamical processes with consideration of three aspects: the structures of complex layered networks, the asymmetrically interacting spreading dynamics, and the timing of the two types of spreading dynamics. When these three aspects are considered simultaneously, an epidemic outbreak on the physical layer can induce an outbreak on the communication layer, and information dissemination can effectively enhance the epidemic threshold. On that basis, Wang et al. [Wang, Liu, Cai et al. (2016)] further investigated the coevolution mechanisms and dynamics between information and disease spreading by utilizing real data and a proposed spreading model on multiplex network. The previous studies usually suppose that all aware individuals take the same level of precautions, ignoring individual heterogeneity. Kan et al. [Kan and Zhang (2017)] proved that though the introduction of the self-awareness can decrease the density of infection, which cannot increase the epidemic threshold no matter of the local or global information. Their finding is remarkably different to many previous results on single-layer network: local information based behavioral response can change the epidemic threshold. Pan et al. [Pan and Yan (2018)] investigated the coupled awareness-epidemic dynamics in multiplex networks considering individual heterogeneity. In Zang [Zang (2018)], a global awareness controlled spreading model (GACS) was proposed to explore the interplay between the coupled dynamical processes. To get a better understanding of the different roles of the spreading scope and effectiveness, Li et al. [Li, Liu, Peng et al. (2018)] proposed an epidemic model on multiplex networks with link overlapping.

Although significant progress has been made in the study of complicated interplay between information dissemination and disease spreading, most of the studies presented so far refer to cases where the epidemic spreading takes place over a static network. The wiring structures of physical connections between individuals are fixed in time, or grown, once forever. The dynamics of epidemic spreading and the properties of final state are in fact heavily influenced by the network topology or connectivity patterns [Pastor-Satorras and Vespignani (2001);taba Gross, D'Lima and Blasius (2006); Frasca, Buscarino, Rizzo et al. (2006); Buscarino, Fortuna, Frasca et al. (2008); Li, Cao and Cao (2010); Buscarino, Fortuna, Frasca et al. (2014)]. A more reasonable setting is to consider the physical contact networks as dynamical systems, meaning that the wiring structures are allowed to change in time [Gross, D'Lima and Blasius (2006); Frasca, Buscarino, Rizzo et al. (2006); Buscarino, Fortuna, Frasca et al. (2008); Li, Cao and Cao (2010); Buscarino, Fortuna, Frasca et al. (2014)].

Here we focus on the interplay between information and disease spreading in multiplex networks of moving agents. The multiplex networks are composed of two layers of networks: one is static communication network where the information dissemination process takes place, and the other is dynamical disease spreading network consisting of a time-evolving wiring of interactions among a group of random walkers. This setting of

multilayer network conforms to the scenario, where the connections of communication layer are always fixed in a period of time but the physical connections of contact layer are changed in time and space. For example, people have a series of physical contacts due to daily activities on both short-range (commuting) and long-range (leisure or business trips) movements, while they can maintain stable social relationships at long durations. This stable number of relationships can be traced back to Dunbar's Number in the 1990s. Dunbar's theory contends that the human brain is only capable of managing relationships (staying in contact at least once per year and knowing how friends relate to others) with about 150 friends, which means that people seldom meet new friends and keep in touch with them in a short time. Therefore, the communication connections are assumed to be static in the information network and the physical connections are assumed to be time-varying in the disease network.

The remainder of this paper is arranged as follows. Section 2 describes the construction of the double-layer network, introduces the new model characterizing the coupled dynamics between information dissemination and disease spreading in populations of moving agents. In Section 3, the Monte Carlo simulations are performed to characterize the interaction process between information and disease spreading and investigate factors that influence spreading dynamics. The conclusions are given in Section 4.

2 Model for information and disease spreading

The multiplex network for information and disease spreading formed by two layers is depicted in Fig. 1. The top layer (denoted by A) is a representation of a static communication network, while the bottom one (denoted by B) is formed by the dynamical network of physical contacts. All nodes represent the same individuals in both layers, and each node of layer A is matched one-to-one with that of layer B. Each layer possesses a different topology, and the dynamical processes of disease and information spreading are typically asymmetrically coupled with each other.

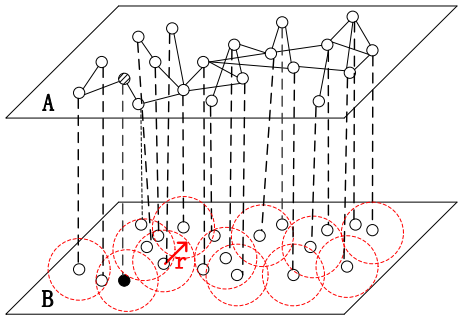

Figure 1: Multiplex network for information and disease spreading (each node of layer A is matched one-to-one with that of layer B)

On top of the communication layer (layer A), we refer to Wang's model of asymmetrically interacting spreading dynamics [Wang, Tang, Yang et al. (2014)] adopting classic susceptible-infected-recovered (SIR) model [Moreno, Pastor-Satorras and Vespignani (2002)] to describe the dissemination of information about the disease. Each node of layer A can be in one of the three states: susceptible state (SA), informed

state (IA), and recovered state (RA), where A represents layer A. Here, SA stands for the people who never heard or received any information about the disease (similar to ignorants), IA stands for the people who are aware of disease and are capable of transmitting the information to others in the same layer (similar to information spreaders), and RA stands for the people who have received the information but are not willing to pass it on to others (similar to stiflers). The process of node state transfer is shown in Fig. 2 on the left. At each time step, information in layer A can come from two sources, the communication with informed neighbors of layer A or because the corresponding individual in layer B is already infected. If a neighbor is in the susceptible state, it will be informed with probability β_A which can be called information-transmission rate. At the same time, each informed node can enter the recovering phase with probability μ_A which can be called information-recovery rate. Once an informed node makes a transition to the recovered state, it will remain in this state for all subsequent time.

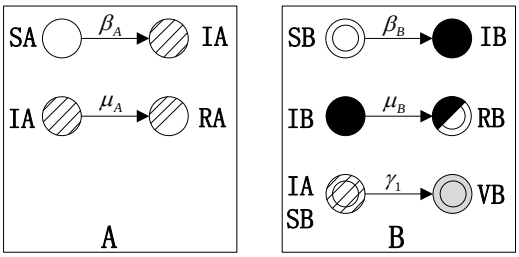

Figure 2: The processes of node state transfer on layers A and B

In the physical layer B, the spreading dynamics of (susceptible-infected-recovered-vaccinated) SIRV model [Wang, Tang, Yang et al. (2014)] can be used to describe the disease spreading process. Each node of layer B can be in one of the four states: Susceptible state (SB), infected state (IB), recovered state (RB), and vaccinated state (VB), where B represents layer B. The process of node state transfer is shown in Fig. 2 on the right. The disease spreads from infected individuals to their neighbors with a probability β_B which can be called disease-transmission rate, and infected individuals eventually recover with probability μ_B which can be called disease-recovery rate. If a node in layer B is in the susceptible state but its counterpart node in layer A is in the informed state, the node in layer B will be vaccinated with probability γ_1 which can be called vaccination rate.

Since people in the realistic life are allowed to move, we employ dynamical network model [Frasca, Buscarino, Rizzo et al. (2006); Buscarino, Fortuna, Frasca et al. (2008); Buscarino, Fortuna, Frasca et al. (2014)] to describe the network topology of contact layer B. Precisely, the individuals constituting the nodes of the physical layer are here random walkers, which may additionally perform long-distance jumps and are only able to interact with individuals falling within a given interaction radius apart from them. The interaction radius r (denoted in Fig. 1) is defined in layer B, where each individual interacts at a given time with only those individuals located within a neighborhood of radius r. Referring to the construction of dynamical network model [Frasca, Buscarino,

Rizzo et al. (2006); Buscarino, Fortuna, Frasca et al. (2008); Buscarino, Fortuna, Frasca et al. (2014)], we consider a system of N identical individuals independently moving in a two-dimensional plane of linear size L, with periodic boundary conditions. The individuals are represented as point particles, and their positions and velocities at time t are denoted as $\mathbf{r}_i(t)$ and $\mathbf{v}_i(t) \equiv (v_i(t)\cos\theta_i(t), v_i(t)\sin\theta_i(t))$, $i = 1,...,N$. In our model, we further assume that the individuals move with a velocity modulus which is constant in time and equal for all the agents, i.e. $v_i(t) = v, \forall i = 1,...,N$ and $\forall t$. At the initial time $t = 0$ the N particles were distributed at random. At each time step, the individuals are random walkers that update stochastically the direction angles $\theta_i(t)$. The position and the orientation of each particle are updated according to Frasca et al. [Frasca, Buscarino, Rizzo et al. (2006); Buscarino, Fortuna, Frasca et al. (2008); Buscarino, Fortuna, Frasca et al. (2014)]

$$\begin{aligned} \mathbf{r}_i(t+\Delta t) &= \mathbf{r}_i(t) + \mathbf{v}_i(t)\Delta t \\ \theta_i(t+\Delta t) &= \xi_i(t+\Delta t) \end{aligned} \tag{1}$$

where $\xi_i(t)$ are N independent identically distributed random variables chosen at each time with uniform probability in the interval $[-\pi, \pi]$. Additionally, to make the movements of individuals include the possibility that particles can move through the bidimensional space with time scales much shorter than those related to disease, as in the real scenario of individuals travelling by flights [Colizza, Barrat, Barthélemy et al. (2006)], we take into account that particle can make a long-distance jump with probability $p_{jump} \in [0,1]$. The parameter p_{jump} quantifies the probability for a particle to perform a long-range jump into a completely random position, far from its previous position. In summary, at each time step, each particle moves following Eq. (1) (where $\mathbf{v}_i(t) \equiv (v\cos\theta_i(t), v\sin\theta_i(t))$) with a probability $1 - p_{jump}$, or performing a jump with probability p_{jump}. In the latter case Eq. (1) with $\mathbf{v}_i(t) \equiv (v_M \cos\theta_i(t), v_M \sin\theta_i(t))$, where $v/v_M = 0.03$, are used. As can be seen from the above, $\rho = N/L^2$, r, v, and p_{jump} are the main parameters to influence the contact network topology of layer B with moving individuals.

Combined with the movement of individuals, the interaction processes between information dissemination and disease spreading can be summarized as follows. First, at time $t = 0$, a small number of nodes in layer B is randomly set as the seed of the infection, and the counterparts in layer A gain simultaneously the information that they are infected by disease. All other pairs of nodes, one from layer A and another from layer B, both are in the susceptible state. Then, at each time step, information dissemination obeys the SIR dynamical process in layer A, and the disease spreading follows the SIRV dynamical process in layer B. For a given individual in layer B, the probability of being infected increases with the number of infected individuals in the neighborhood of radius r. In layer B, we assume that the infection lasts $\tau = 1/\mu_B$ simulation steps, so that all infected individuals become recovered τ simulation steps after having transformed into infected state and, after that time τ, they cannot catch the disease anymore. After that, the position and the orientation of each particle are updated according to Eq. (1). Finally, the

interaction spreading dynamics terminate, since all infected or informed nodes in both layers become recovered states that can no longer infect others.

Next, we use microscopic Markov chain approach (MMCA) to establish the MMCA equations characterizing the coupled dynamics between information and disease spreading. Let A denote the adjacency matrix representing the topological graph $G^A=(V^A,E^A)$ of layer A, i.e. $a_{ij}=1$ if $(i,j)\in E^A$ and $a_{ij}=0$ otherwise. At time k, each node i can be in one of three possible states: SA, IA, and RA. The state of the node is indicated by a status vector $\mathbf{s}_i^A(k)$, where a single 1 in the position corresponding to the present state, and 0 everywhere else. $\mathbf{s}_i^A(k)=[s_i^{SA}(k)s_i^{IA}(k)s_i^{RA}(k)]^T$, for all $i\in 1,...,N$.

Let $\mathbf{p}_i^A(k)=[p_i^{SA}(k)p_i^{IA}(k)p_i^{RA}(k)]^T$ be the probability mass function (PMF) of node i at time k. For every node i it states the probability of being in each of the possible states at time k. Moreover, let $B(k)$ denote the interaction matrix of layer B at time $t=k$, as the connections of contact layer B change over time. $b_{ij}(k)=1$ if the jth node is within the interaction radius of the ith node at time $t=k$, and $b_{ij}(k)=0$ otherwise (Especially, it is assumed that $b_{ii}(k)=1,\ \forall i=1,...,N$).

The evolution of SIR in layer A is described by the following equations:

$$\begin{aligned}
&p_i^{SA}(k+1)=s_i^{SA}(k)[1-f_i^A(k)-g_i^B(k)]\\
&p_i^{IA}(k+1)=s_i^{SA}(k)[f_i^A(k)+g_i^B(k)]+(1-\mu_A)s_i^{IA}(k)\\
&p_i^{RA}(k+1)=s_i^{RA}(k)+\mu_A s_i^{IA}(k)\\
&\mathbf{s}_i^A(k+1)^T=\text{MultiRealize}[\mathbf{p}_i^A(\text{k+1})^T]
\end{aligned} \tag{2}$$

where MultiRealize$[\bullet]$ performs a random realization for the PMF given with $\mathbf{p}_i^A$(k+1). In the model, $f_i^A(k)$ is the probability that a susceptible individual i receives the information from any combination of its informed neighbors at time $t=k$, and $g_i^B(k)$ is the probability that a susceptible individual i catches the disease from any contact of its infected individuals in the neighborhood of radius r at time $t=k$. $f_i^A(k)$ and $g_i^B(k)$ are given by

$$\begin{aligned}
&f_i^A(k)=1-\prod_{j=1}^{N}[1-\beta_A a_{ij}s_j^{IA}(k)]\\
&g_i^B(k)=1-\prod_{j=1}^{N}[1-\beta_B b_{ij}(k)s_j^{IB}(k)]
\end{aligned} \tag{3}$$

Let $X^A(k)=\sum_{i=1}^{N}s_i^{SA}(k)$, $Y^A(k)=\sum_{i=1}^{N}s_i^{IA}(k)$, and $Z^A(k)=\sum_{i=1}^{N}s_i^{RA}(k)$ be the total number of nodes in statuses SA, IA, and RA at time $t=k$, respectively. Further, let $N_1^A=\text{E}[X^A(\infty)]$, $N_2^A=\text{E}[Y^A(\infty)]$, and $N_3^A=\text{E}[Z^A(\infty)]$ be the average number of nodes that eventually (when $k\to\infty$) adopt statues SA, IA, and RA, respectively.

In the following, we rewrite the model given with Eqs. (2) and (3) as Eqs. (4) and (5) to facilitate the mathematical analysis.

$$\begin{aligned} p_i^{SA}(k+1) &= p_i^{SA}(k)[1-f_i^A(k)-g_i^B(k)] \\ p_i^{IA}(k+1) &= p_i^{SA}(k)[f_i^A(k)+g_i^B(k)]+(1-\mu_A)p_i^{IA}(k) \\ p_i^{RA}(k+1) &= p_i^{RA}(k)+\mu_A p_i^{IA}(k) \end{aligned} \tag{4}$$

$$\begin{aligned} f_i^A(k) &= 1-\prod_{j=1}^{N}[1-\beta_A a_{ij} p_j^{IA}(k)] \\ g_i^B(k) &= 1-\prod_{j=1}^{N}[1-\beta_B b_{ij}(k) p_j^{IB}(k)] \end{aligned} \tag{5}$$

Equivalently N_1^A, N_2^A, and N_3^A can be calculated using Eq. (4) as $N_1^A=\sum_{i=1}^{N} p_i^{SA}(\infty)$, $N_2^A=\sum_{i=1}^{N} p_i^{IA}(\infty)$, and $N_3^A=\sum_{i=1}^{N} p_i^{RA}(\infty)$.

Similarly, The MMCA equations describing the evolution of SIRV dynamics in layer B are

$$\begin{aligned} p_i^{SB}(k+1) &= p_i^{SB}(k)[1-g_i^B(k)-\gamma_1 p_i^{SA}(k) f_i^A(k)] \\ p_i^{IB}(k+1) &= p_i^{SB}(k) g_i^B(k)+(1-\mu_B)p_i^{IB}(k) \\ p_i^{RB}(k+1) &= p_i^{RB}(k)+\mu_B p_i^{IB}(k) \\ p_i^{VB}(k+1) &= p_i^{VB}(k)+\gamma_1 p_i^{SB}(k) p_i^{SA}(k) f_i^A(k) \end{aligned} \tag{6}$$

In the above, p_i^{SB}, p_i^{IB}, p_i^{RB}, and p_i^{VB} are the probability of node i at time k which are in the susceptible state, infected state, recovered state and vaccinated state, respectively. μ_B and γ_1 respectively denote the disease-recovery rate and vaccination rate in layer B. $f_i^A(k)$ and $g_i^B(k)$ are given by Eq. (5).

3 Simulation results

Modeling double-layer network needs to establish topology of each layer. The top layer A stands for the virtual communication network for delivering information among agents. We adopt BA scale-free network model to generate a network consisting of 1000 nodes ($N=1000$). The average degree of the generated network is 6 ($\langle k\rangle=6$). Relevant characteristic parameters of network topology are listed in Tab. 1.

Table 1: The characteristic parameters of double-layer network consisting of network A and network B

Layer	Network Model	Network Size N	Average Degree $\langle k \rangle$	Average Path Length $\langle d \rangle$
A	BA network	1000	6	3.48
B	time-varying network	1000	3.14	6.69

Connections of nodes in network A are shown in Fig. 3(a). Considering individuals' random walk, we adopt the construction methods of time-varying networks [Frasca, Buscarino, Rizzo et al. (2006); Buscarino, Fortuna, Frasca et al. (2008); Buscarino, Fortuna, Frasca et al. (2014)] to establish network B (layer B). To be one-to-one correspondence between nodes of network A and nodes of network B, we also set the size of network B $N=1000$. The density of nodes in two-dimensional plane is $\rho=1$. In network B, the interaction radius among nodes is $r=1$, namely, the average degree is $\langle k \rangle = \pi r^2 \approx 3.14$. Relevant characteristic parameters of network B can be seen in Tab. 1. The links in network B meeting periodic boundary conditions are shown in Fig. 3(b). Calculated by formula $\rho = N/L^2$, the width of two-dimensional plane in network B is $L=\sqrt{N/\rho}=\sqrt{1000}\approx 31.62$, which is the length of horizontal axis in Fig. 3(b). Actually, to be one-to-one correspondence between nodes of network A and nodes of network B visually, we also set network A is a two-dimensional plane with the same $L\approx 31.62$. At the initial time $t=0$, the coordinates of nodes in both A and B are set randomly by formula $L*rand(1,1)$.

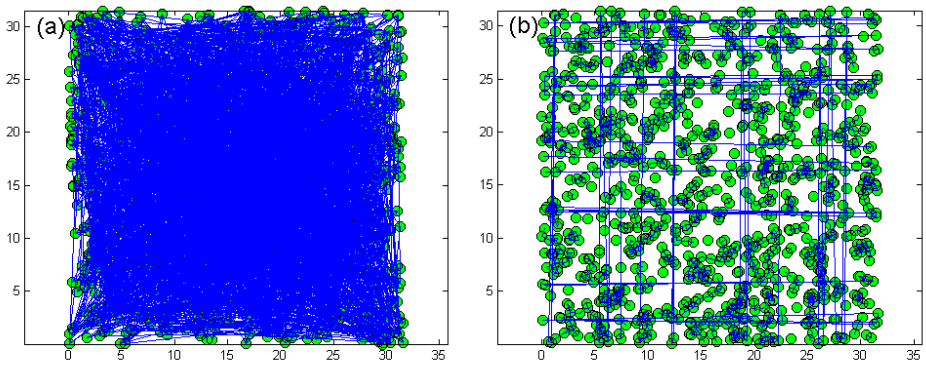

Figure 3: Connections diagram of double-layer network at the initial time (a) Connections of nodes in network A, (b) Connections of nodes in network B

Next, on the basis of the proposed interaction spreading model, we analyze the factors that influence the interaction between information and disease considering the following two scenarios.

3.1 First scenario

Firstly, as the description of Eqs. (4) and (6), susceptible individuals of layer B will vaccinate with probability γ_1 and become vaccinated state VB immediately after receiving information about disease spreading. Initially, the proportion of infected nodes in layer B is set to 2%. At each time step, information dissemination obeys the SIR dynamical process in layer A, and the disease spreading follows the SIRV dynamical process in layer B.

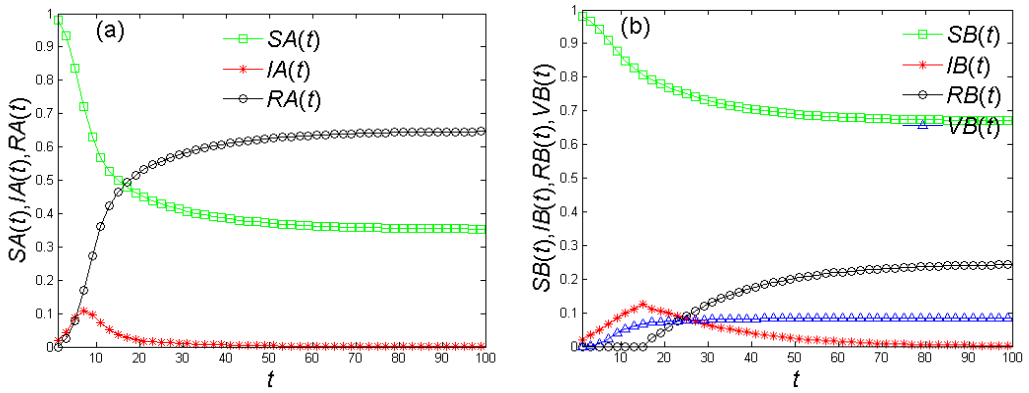

Figure 4: Evolution processes of information dissemination and disease spreading on double-layer network. (a) Information dissemination in layer A, (b) Disease spreading in layer B

The evolution process of information dissemination in layer A is shown in Fig. 4(a) and that of disease spreading in layer B is shown in Fig. 4(b). Relevant parameters are set as follows $\beta_A = 0.1$, $\mu_A = 0.5$, $\beta_B = 0.1$, $\tau = 15$, $\gamma_1 = 0.1$, $r = 1$, $\rho = 1$, $v = 0.03$, $p_{jump} = 0$.

Fig. 4(a) shows that the density of susceptible individuals ($SA(t)$) in network A decreases with time until the propagation process reaches the steady state. The density of individuals under the informed state ($IA(t)$) (information spreaders) increases firstly and then decreases to zero over time, which embodies so-called lifecycle of information propagation. The density of recovered individuals ($RA(t)$) increases gradually until the propagation process reaches the steady state, where $RA(t)$ tends to be a constant value called information dissemination range.

In network B, the evolution process of disease spreading is shown in Fig. 4(b). The density of susceptible individuals ($SB(t)$) decreases with time until the spreading process reaches the steady state. The density of infected individuals ($IB(t)$) (disease spreaders) increases firstly and then decreases slowly to zero over time. The density of recovered individuals ($RB(t)$) initially keeps zero for a certain time, and then increases rapidly from zero to a

constant value over time. This constant value is called disease spreading scale. The density of individuals under vaccinated state ($VB(t)$) is affected by the information dissemination in network A, which $VB(t)$ no longer increases with extinction of individuals under the informed state ($IA(t)$). In network B, the recovery time step of infected individuals is set as $\tau = 15$, which causes the transition in the evolution of recovered individuals ($RB(t)$) from $t = 1$ to $t = 16$. When susceptible individuals turn to be infected ones, they will become recovered after τ time steps ($\tau = 15$). In network B, the density of individuals under vaccinated state ($VB(t)$) increases just in a short time, and then it keeps a constant value. This is because susceptible individual in network B become vaccinated state with the probability γ_1 only when the counterpart in network A is under the informed state. $IA(t)$ increases in a short time and decreases to zero quickly, which triggers a brief increase of the density of vaccinated individuals $VB(t)$.

Table 2: The characteristic parameters of double-layer network consisting of network A and network B

Layer	Varying Parameter	Other Parameters	Figure
Layer A	$\beta_A = 0.1, 0.3, 0.5$	$\mu_A = 1, \beta_B = 0.1, \tau = 15, \gamma_1 = 0.1, r = 1,$ $\rho = 1, p_{jump} = 0, v = 0.03$	Fig. 5
Layer A	$\mu_A = 0.5, 0.7, 1$	$\beta_A = 0.1, \beta_B = 0.1, \tau = 15, \gamma_1 = 0.1, r = 1,$ $\rho = 1, p_{jump} = 0, v = 0.03$	Fig. 6
Layer B	$\beta_B = 0.1, 0.3, 0.5$	$\mu_A = 1, \beta_A = 0.1, \tau = 15, \gamma_1 = 0.1, r = 1,$ $\rho = 1, p_{jump} = 0, v = 0.03$	Fig. 7
Layer B	$\gamma_1 = 0.1, 0.3, 0.5$	$\mu_A = 1, \beta_A = 0.1, \beta_B = 0.1, \tau = 15, r = 1,$ $\rho = 1, p_{jump} = 0, v = 0.03$	Fig. 8
Layer B	$\gamma_1 = 0.1, 0.3, 0.5$	$\mu_A = 0.5, \beta_A = 0.1, \beta_B = 0.1, \tau = 15, r = 1,$ $\rho = 1, p_{jump} = 0, v = 0.03$	Fig. 9
Layer B	$\tau = 1/\mu_B = 5, 10, 15$	$\mu_A = 0.3, \beta_A = 0.1, \beta_B = 0.1, \gamma_1 = 0.1,$ $r = 1, \rho = 1, p_{jump} = 0, v = 0.03$	Fig. 10
Layer B	$p_{jump} = 0.1, 0.3, 0.5$	$\mu_A = 0.5, \beta_A = 0.1, \beta_B = 0.1, \tau = 15,$ $\gamma_1 = 0.1, r = 1, \rho = 1, v_M = 1$	Fig. 11

Next, we will analyze the factors that influence the information and disease spreading respectively. How relevant parameters influence the information and disease spreading is showed in simulation figures. Tab. 2 shows the correspondence between parameters and

relevant simulation figures, where $\tau = 1/\mu_B$. Other parameters are set as shown in the third column of Tab. 2. The initial infection density in layer B is 2%.

(1) How information-transmission rate β_A influences information and disease spreading?

Fig. 5 shows the evolution processes of information and disease spreading in double-layer network with different β_A . Figs. 5(a) and (b) show the density evolution curves of informed and recovered individuals in layer A respectively. In Fig. 5(a), we can see that the larger the β_A is, the higher the peak value of the density of information spreaders is. According to the Fig. 5(b), it can be seen that the larger the β_A is, the larger the information dissemination range is, which indicates that the information is widely transmitted. In addition, the peak value of the density of information spreaders and the dissemination range rise prominently as β_A increases. According to the rule of interaction between information and disease spreading, if the number of information spreaders increases, correspondingly the number of vaccinated individuals in layer B will increase and disease spreading will be inhibited to some extent. However, in Fig. 5(c), the peak value of the density of disease spreaders does not decrease remarkably as β_A increases. Besides, from Fig. 5(d), we can see that the disease spreading scale in layer B doesn't decrease remarkably as well when β_A increases from 0.3 to 0.5.

Therefore, increasing information-transmission rate can enhance the peak value of the density of information spreaders and scale up the dissemination range of information in communication layer A. It can also reduce the scale of disease spreading. However, when the information-transmission rate is increased to a certain value, the effect of inhibiting disease spreading is particularly weak.

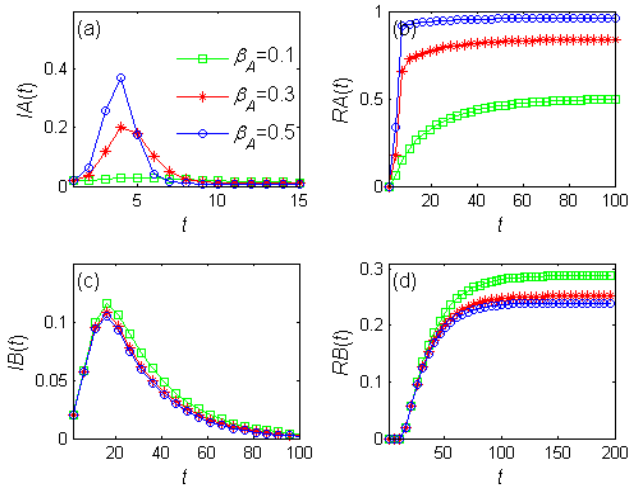

Figure 5: The evolution processes of information and disease in double-layer network with different β_A . (a) The density of information spreaders in layer A, (b) The density of recovered individuals in layer A, (c) The density of disease spreaders in layer B, (d) the density of recovered individuals in layer B

(2) How the information-recovery rate μ_A influences information and disease spreading?

Fig. 6 shows the evolution processes of information and disease spreading in double-layer network with different μ_A. Figs. 6(a) and 6(b) show the density evolution curves of informed and recovered individuals in layer A respectively. From Fig. 6(a) we can see that the smaller the μ_A is, the higher the peak value of the density of information spreaders is. According to the Fig. 6(b), it can be seen that the smaller the μ_A is, the larger the information dissemination range is. When μ_A decreases from 1 to 0.5, the density peak value of information spreaders increases from 0.03 to 0.107 and the information dissemination scale increases from 0.5 to 0.648. In Fig. 6(c), the peak value of the density of disease spreaders decreases from 0.129 to 0.125, which is not obvious. In Fig. 6(d), two curves denoting μ_A=0.7 and μ_A=1 are adjacent.

Therefore, decreasing information-recovery rate can enhance the peak value of the density of information spreaders and scale up the dissemination range of information in communication layer A, while the scale increment is small. Also, it can reduce the scale of disease spreading to a certain degree.

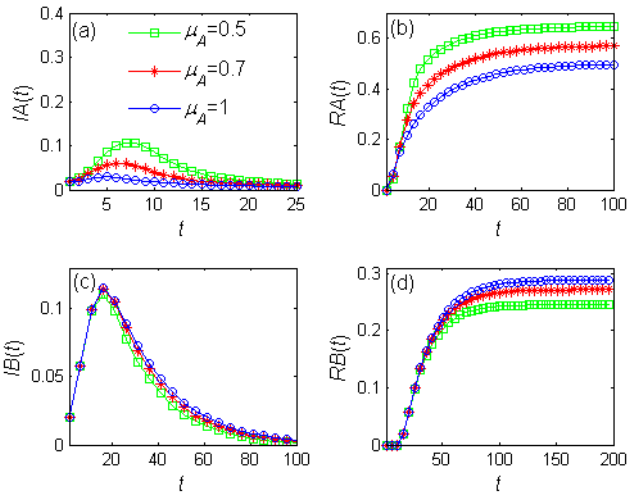

Figure 6: The evolution processes of information and disease in double-layer network with different μ_A. (a) The density of information spreaders in layer A. (b) The density of recovered individuals in layer A. (c) The density of disease spreaders in layer B. (d) The density of recovered individuals in layer B

(3) How the disease-transmission rate β_B influences information and disease spreading?

Fig. 7 shows the evolution processes of information and disease spreading in double-layer network with different β_B. Figs. 7(a) and 7(b) show the density evolution curves of informed and recovered individuals in layer A respectively. We can see that when β_B increases from 0.1 to 0.5, the peak value of the density of information spreaders increases from 0.03 to 0.07 and the information dissemination scale increases from 0.5 to 0.71. As

can be seen from the Figs. 7(c) and 7(d), with the increase of β_B, the peak value and scale of disease spreading are increased obviously. Hence, increasing disease-transmission rate can not only increase the peak value and scale of disease spreading, but also increase the peak value and scale of information dissemination.

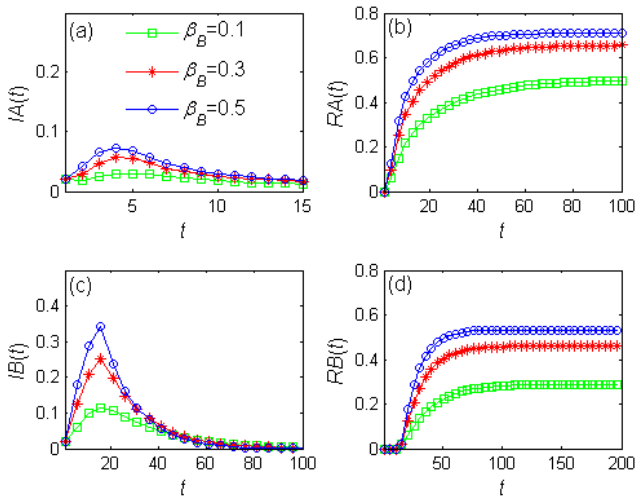

Figure 7: The evolution processes of information and disease in double-layer network with different β_B. (a) The density of information spreaders in layer A. (b) The density of recovered individuals in layer A. (c) The density of disease spreaders in layer B. (d) The density of recovered individuals in layer B

(4) How the vaccination rate γ_1 influences information and disease spreading?

Fig. 8 shows the evolution processes of information and disease spreading in double-layer network with different γ_1. Figs. 8(a) and 8(b) show the density evolution curves of informed and recovered individuals in layer A respectively. We can see that when γ_1 increases from 0.1 to 0.5, the peak value of the density of information spreaders is almost constant and the information dissemination scale reduces from 0.5 to 0.447. As can be seen from the Figs. 8(c) and 8(d), with the increase of γ_1, the peak value of disease spreading decreases from 0.129 to 0.119, and the scale of disease spreading decreases from 0.289 to 0.233.

Besides, Fig. 9 shows the evolution processes of information and disease spreading in double-layer network with different γ_1 where μ_A=0.5. According to the Fig. 8 and Fig. 9, it can be seen that the disease spreading scale decreases as γ_1 increases, which conforms with the actual situation that increasing vaccination rate can reduce the scale of disease spreading. In addition, when μ_A is set to 0.5 and 1 respectively, the influence on information and disease spreading is coincident with the above analysis (2).

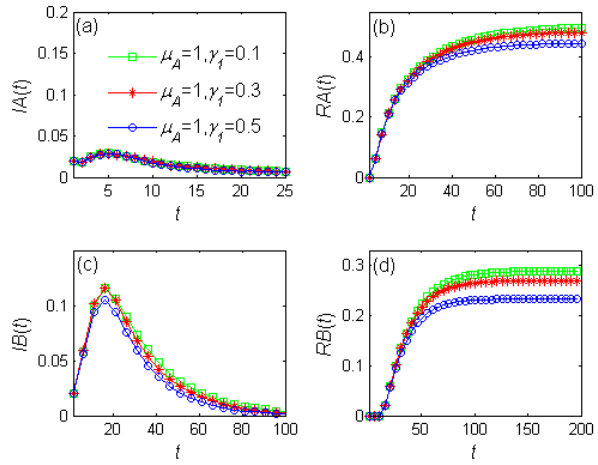

Figure 8: The evolution processes of information and disease in double-layer network where γ_1 changes and μ_A=1. (a) The density of information spreaders in layer A. (b) The density of recovered individuals in layer A. (c) The density of disease spreaders in layer B. (d) The density of recovered individuals in layer B

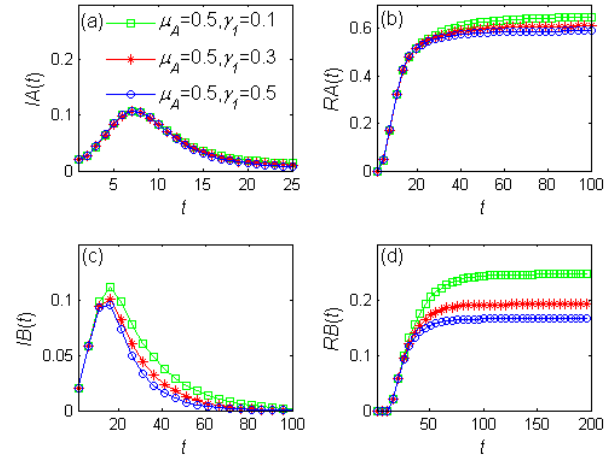

Figure 9: The evolution processes of information and disease in double-layer network where γ_1 changes and μ_A=0.5. (a) The density of information spreaders in layer A. (b) The density of recovered individuals in layer A. (c) The density of disease spreaders in layer B. (d) The density of recovered individuals in layer B

(5) How the time step of keeping infected (infection period) $\tau = 1/\mu_B$ influences information and disease spreading?

Fig. 10 shows the evolution processes of information and disease spreading in double-layer network with different τ. Figs. 10(a) and 10(b) show the density evolution curves of informed and recovered individuals in layer A respectively. The different time steps account for the different infection periods. We can see that when the time step increases

from 5 to 15, the peak value of the density of information spreaders is almost constant, and the information dissemination scale increases from 0.775 to 0.839, which changes little. In Fig. 10(c), with the increase of τ, the peak value of disease spreading increases from 0.103 to 0.246 and the time to reach the peak value is increasing. Similarly, in Fig. 10(d), the scale of disease spreading increases from 0.243 to 0.352 and the time to reach the steady state also gets longer as τ increases.

Therefore, longer infection period leads to larger peak value and wider scale of disease spreading. Also, the time to reach the peak value and the steady state gets longer. However, the infection period has little influence on the information dissemination in communication layer A.

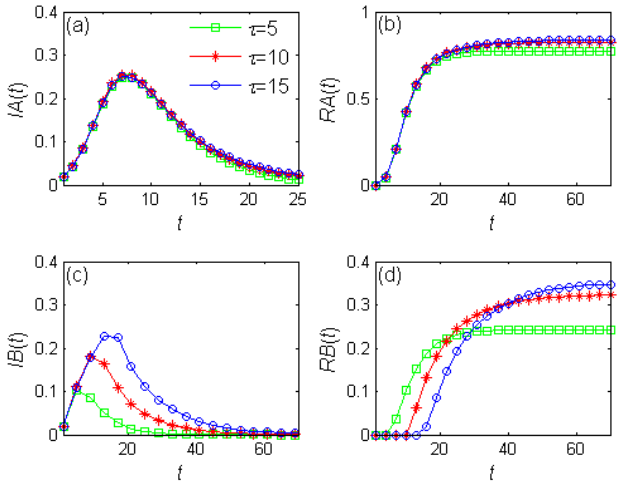

Figure 10: The evolution processes of information and disease in double-layer network with different τ. (a) The density of information spreaders in layer A. (b) The density of recovered individuals in layer A. (c) The density of disease spreaders in layer B. (d) The density of recovered individuals in layer B

(6) How the probability of performing a long-range jump p_{jump} influences information and disease spreading?

Fig. 11 shows the evolution processes of information and disease spreading in double-layer network with different p_{jump}. Figs. 11(a) and 11(b) show the density evolution curves of informed and recovered individuals in layer A respectively. We can see that the density of information spreaders and the information dissemination scale both increase as p_{jump} increases. In Figs. 11(c) and 11(d), with the increase of p_{jump}, the peak value of disease spreading rises from 0.183 to 0.419 and the disease spreading scale rises from 0.635 to 0.863. Therefore, increasing the probability of performing a long-range jump will not only increase the peak value and scale of disease spreading, but also increase the information dissemination scale in communication layer A. Additionally, from Fig. 11(c) we can see that increasing the probability of performing a long-range jump can accelerate the extinction of disease spreaders, accelerating the spread of disease. In fact, it is because

the probability p_{jump} influences the statistical properties of dynamical contact network topology consisting of moving individuals [Frasca, Buscarino, Rizzo et al. (2006)].

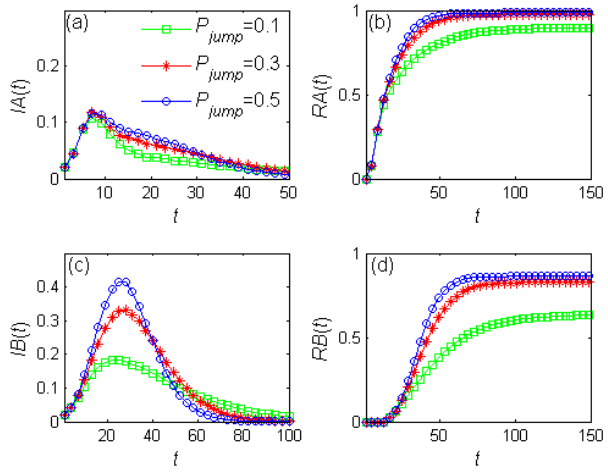

Figure 11: The evolution processes of information and disease in double-layer network with different p_{jump}. (a) The density of information spreaders in layer A. (b) The density of recovered individuals in layer A. (c) The density of disease spreaders in layer B. (d) The density of recovered individuals in layer B

Fig. 12 and Fig. 13 respectively show the average path length $L_G(t)$ and average degree $\langle k\rangle_G(t)$ of dynamical contact network topology (layer B) with different probability p_{jump}. $G(t)$ denotes the adjacent matrix of dynamical contact network and describes the contacts situation of individuals during the whole infection period ($t=1,...,T-\tau+1$). At each time step, the adjacent matrix of network B is time-varying. Let $B(t)$ denote the adjacent matrix of layer B at time t, and the element of adjacent matrix is denoted by $b_{ij}(t)$. $b_{ij}(t)=1$ if the jth node is within the interaction radius of the ith node at time t, and $b_{ij}(t)=0$ otherwise (Especially, it is assumed that $b_{ii}(t)=1$, $\forall i=1,...,N$). For $t=1,...,T-\tau+1$, $g_{ij}(t)=1$ if at least for one k (with $k=t,...,t+\tau-1$) it is verified that $b_{ij}(k)=1; g_{ij}(t)=0$ otherwise. As can be seen from the Fig. 12 and Fig. 13, with the increase of probability p_{jump}, the average path length $L_G(t)$ of dynamical contact network decreases, while the average degree $\langle k\rangle_G(t)$ increases. Namely, the number of contacts among individuals is increasing, which fully explains why increasing the probability of performing a long-range jump can increase the peak value and scale of disease spreading. Therefore, to avoid widespread of disease, people should reduce the frequency of long-range travel when faced with epidemic spreading.

3.2 Second Scenario

Secondly, we consider that susceptible individuals reduce the range of movement with the probability γ_2 to prevent disease when being informed of disease spreading. Namely, susceptible individuals in layer B reduce the interaction radius r with the probability γ_2, if the corresponding nodes in layer A are under the informed state (IA).

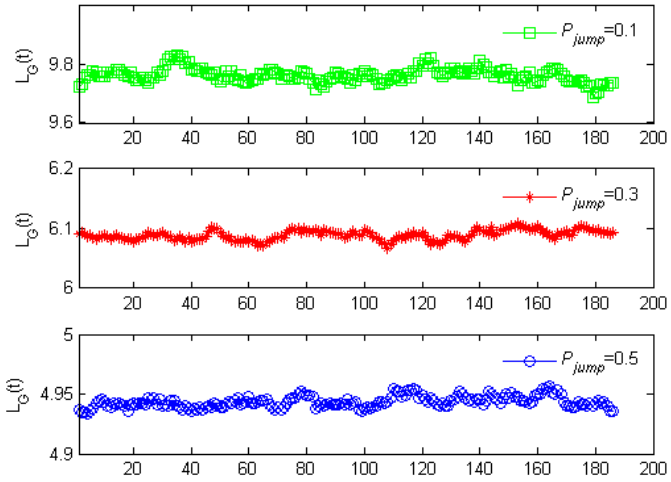

Figure 12: The average path length $L_G(t)$ of dynamical contact network topology with different probability p_{jump}

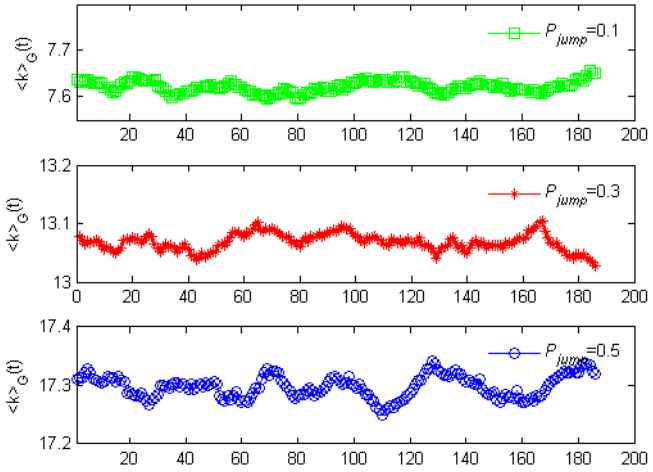

Figure 13: The average degree $\langle k\rangle_G(t)$ of dynamical contact network topology with different probability p_{jump}

Fig. 14 shows the evolution processes of information and disease spreading in double-layer network with different γ_2. Other parameters are set as the interaction radius $r=0.5$,

$\beta_A = 0.2$, $\mu_A = 0.3$, $\beta_B = 0.3$, $\tau = 15$, $\rho = 1$, $\nu = 0.03$, $p_{jump} = 0$. Initially, the density of infected individuals in layer B is still 2%. Fig. 14(a) and 14(b) show the density evolution curves of informed and recovered individuals in layer A respectively. We find that the peak value and scale of information dissemination almost keep unchanged when γ_2 increases from 0.1 to 1. The increase of γ_2 accounts for strengthening consciousness for self-protection. From Figs. 14(c) and 14(d), we can see that the peak value of disease spreading decreases from 0.268 to 0.211 and the disease spreading scale decreases from 0.509 to 0.237 when γ_2 increases from 0.1 to 1.

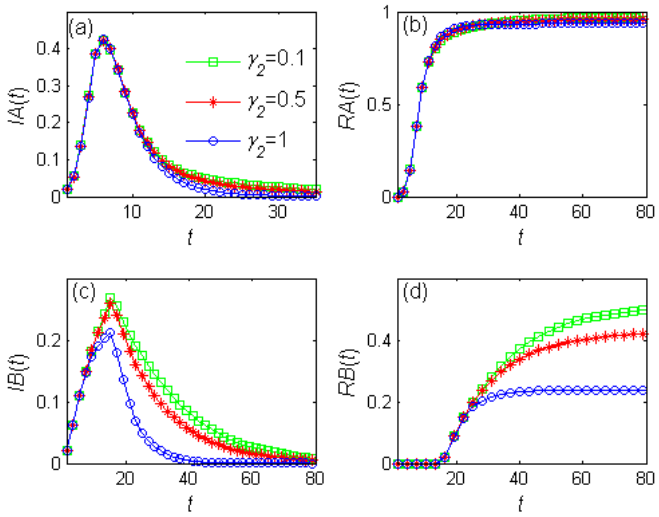

Figure 14: The evolution processes of information and disease in double-layer network with different γ_2 . (a) The density of information spreaders in layer A. (b) The density of recovered individuals in layer A. (c) The density of disease spreaders in layer B. (d) The density of recovered individuals in layer B

Therefore, strengthening individual prevention consciousness and reducing the scope of activity can effectively decrease the peak value and scale of disease spreading. Meanwhile, it has little influence on the information spreading in communication layer A.

4 Conclusions

This work is mainly focused on the dynamical interaction between information dissemination and disease spreading in populations of moving agents. We have constructed a new double-layer network model, one is static communication network where the information dissemination process takes place, and the other is dynamical disease spreading network consisting of a time-evolving wiring of interactions among a group of random walkers. A new spreading model characterizing the coupled dynamics between information and disease spreading in populations of moving agents is proposed and corresponding state probability equations are formulated to describe the probability in each state of every node at each moment. The Monte Carlo simulations are performed

to characterize the interaction process between information and disease spreading and investigate factors that influence spreading dynamics. Our results show that increasing information-transmission rate and decreasing information-recovery rate both can enhance the peak value of the density of information spreaders and scale up the information dissemination range in communication network, which can also reduce the scale of disease spreading to a certain degree. However, when the information-transmission rate is increased to a certain value, the effect of inhibiting disease spreading is particularly weak. Increasing vaccination rate and shortening infection period both can effectively reduce the scale of disease spreading. In addition, to avoid widespread of disease, people should reduce the frequency of long-range travel and enhance individual prevention consciousness by reducing the scope of activity when faced with epidemic spreading.

Acknowledgement: This research has been supported by the National Natural Science Foundation of China (Grant No. 61672298 and 61373136), the National Social Science Foundation of China (Grant No. 13BTQ046), the High-level Introduction of Talent Scientific Research Start-up Fund of Jiangsu Police Institute (Grant No. JSPI17GKZL403), the Scientific Research Program of Jiangsu Police Institute (Grant No. 2017SJYZQ01), the Science and Technology Plan Projects of Jiangsu Province (Grant No. BE2017067) and the Research Foundation for Humanities and Social Sciences of Ministry of Education of China (Grant No. 15YJAZH016).

References

Bagnoli, F.; Lio, P.; Sguanci, L. (2007): Risk perception in epidemic modeling. *Physical Review E*, vol. 76, no. 6.

Buscarino, A.; Fortuna, L.; Frasca, M.; Latora, V. (2008): Disease spreading in populations of moving agents. *Europhysics Letters*, vol. 82, no. 3.

Buscarino, A.; Fortuna, L.; Frasca, M.; Rizzo, A. (2014): Local and global epidemic outbreaks in populations moving in inhomogeneous environments. *Physical Review E*, vol. 90, no. 4.

Chen, F.; Jiang, M. H.; Rabidoux, S.; Robinson, S. (2011): Public avoidance and epidemics: insights from an economic model. *Journal of Theoretical Biology*, vol. 278, no. 1, pp. 107-119.

Colizza, V.; Barrat, A.; Barthélemy, M.; Vespignani, A. (2006): The role of the airline transportation network in the prediction and predictability of global epidemics. *Proceedings of the National Academy of Sciences of the United States of America*, vol. 103, no. 7, pp. 2015-2020.

Epstein, J. M.; Parker, J.; Cummings, D.; Hammond, R. A. (2008): Coupled contagion dynamics of fear and disease: Mathematical and computational explorations. *PLoS One*, vol. 3, no. 12.

Fenichel, E. P.; Castillo-Chavez, C.; Ceddia, M. G.; Chowell, G.; Parra, P. A. G. et al. (2011): Adaptive human behavior in epidemiological models. *Proceedings of the National Academy of Sciences*, vol. 108, no. 15, pp. 6306-6311.

Frasca, M.; Buscarino, A.; Rizzo, A.; Fortuna, L.; Boccaletti, S. (2006): Dynamical

network model of infective mobile agents. *Physical Review E*, vol. 74, no. 3.

Funk, S.; Gilad, E.; Watkins, C.; Jansen, V. A. A. (2009): The spread of awareness and its impact on epidemic outbreaks. *Proceedings of the National Academy of Sciences*, vol. 106, no. 16, pp. 6872-6877.

Granell, C.; Gómez, S.; Arenas, A. (2013): Dynamical interplay between awareness and epidemic spreading in multiplex networks. *Physical Review Letters*, vol. 111, no. 12.

Granell, C.; Gómez, S.; Arenas, A. (2014): Competing spreading processes on multiplex networks: Awareness and epidemics. *Physical Review E*, vol. 90, no. 1.

Gross, T.; D'Lima, C. J. D.; Blasius, B. (2006): Epidemic dynamics on an adaptive network. *Physical Review Letters*, vol. 96, no. 20.

Jiang, Z. Q.; Xie, W. J.; Li, M. X.; Podobnik, B.; Zhou, W. X. et al. (2013): Calling patterns in human communication dynamics. *Proceedings of the National Academy of Sciences*, vol. 110, no. 5, pp. 1600-1605.

Kan, J. Q.; Zhang, H. F. (2017): Effects of awareness diffusion and self-initiated awareness behavior on epidemic spreading-an approach based on multiplex networks. *Communications in Nonlinear Science and Numerical Simulation*, vol. 44, pp. 193-203.

Li, M.; Liu, R. R.; Peng, D.; Jia, C. X.; Wang, B. H. (2018): Roles of the spreading scope and effectiveness in spreading dynamics on multiplex networks. *Physica A: Statistical Mechanics and Its Applications*, vol. 492, pp. 1239-1246.

Li, X.; Cao, L.; Cao, G. F. (2010): Epidemic prevalence on random mobile dynamical networks: Individual heterogeneity and correlation. *European Physical Journal B*, vol. 75, no. 3, pp. 319-326.

Liu, C.; Xie, J. R.; Chen, H. S.; Zhang, H. F.; Tang, M. (2015): Interplay between the local information based behavioral responses and the epidemic spreading in complex networks. *Chaos: An Interdisciplinary Journal of Nonlinear Science*, vol. 25, no. 10.

Moreno, Y.; Pastor-Satorras, R.; Vespignani, A. (2002): Epidemic outbreaks in complex heterogeneous networks. *European Physical Journal B*, vol. 26, pp. 521-529.

Pan, Y.; Yan, Z. (2018): The impact of multiple information on coupled awareness-epidemic dynamics in multiplex networks. *Physica A: Statistical Mechanics and its Applications*, vol. 491, pp. 45-54.

Pastor-Satorras, R.; Vespignani, A. (2001): Epidemic spreading in scale-free networks. *Physical Review Letters*, vol. 86, no. 14.

Perra, N.; Balcan, D.; Gonçalves, B.; Vespignani, A. (2011): Towards a characterization of behavior-disease models. *PLoS One*, vol. 6, no. 8.

Rizzo, A.; Frasca, M.; Porfiri M. (2014): Effect of individual behavior on epidemic spreading in activity-driven networks. *Physical Review E*, vol. 90, no. 4.

Ruan, Z.; Tang, M.; Liu, Z. (2012): Epidemic spreading with information-driven vaccination. *Physical Review E*, vol. 86, no. 3.

Sahneh, F. D.; Scoglio, C. M. (2012): Optimal information dissemination in epidemic networks. *IEEE 51st Annual Conference on Decision and Control*, pp. 1657-1662.

Starnini, M.; Baronchelli, A.; Pastor-Satorras, R. (2013): Modeling human dynamics

of face-to-face interaction networks. *Physical Review Letters*, vol. 110, no. 16.

Wang, W.; Liu, Q. H.; Cai, S. M.; Tang, M.; Braunstein, L. A. (2016): Suppressing disease spreading by using information diffusion on multiplex networks. *Scientific Reports*, vol. 6.

Wang, W.; Tang, M.; Yang, H.; Do, Y.; Lai, Y. C. et al. (2014): Asymmetrically interacting spreading dynamics on complex layered networks. *Scientific Reports*, vol. 4.

Zang, H. (2018): The effects of global awareness on the spreading of epidemics in multiplex networks. *Physica A: Statistical Mechanics and Its Applications*, vol. 492, no. 4, pp. 1495-1506.

Zhang, H. F.; Xie, J. R.; Tang, M.; Lai, Y. C. (2014): Suppression of epidemic spreading in complex networks by local information based behavioral responses. *Chaos: An Interdisciplinary Journal of Nonlinear Science*, vol. 24, no. 4.